Nanomedicine

DOI: 10.1002/ange.200602471

Designed Fabrication of Multifunctional Magnetic Gold Nanoshells and Their Application to Magnetic Resonance Imaging and Photothermal Therapy**

Jaeyun Kim, Sungjin Park, Ji Eun Lee, Seung Min Jin, Jung Hee Lee, In Su Lee, Ilseung Yang, Jun-Sung Kim, Seong Keun Kim, Myung-Haing Cho, and Taeghwan Hyeon**

Nanotechnology offers tremendous potential for future medical diagnosis and therapy. Various types of nanoparticles have been extensively studied for numerous biomedical applications.[1] Quantum dots modified with tumor-targeting ligands were used as in vivo cancer-targeting imaging agents.[2] Gold nanoparticles derivatized with oligonucleotides were used in an ultrasensitive biobarcode assay.[3]

[*] J. Kim,[§] J. E. Lee, Dr. I. S. Lee, Prof. Dr. T. Hyeon
National Creative Research Initiative Center for Oxide Nanocrystalline Materials and
School of Chemical and Biological Engineering
Seoul National University, Seoul 151-744 (Korea)
Fax: (+82) 2-886-8457
E-mail: thyeon@snu.ac.kr

S. Park,[§] J.-S. Kim, Prof. Dr. M.-H. Cho
Laboratory of Toxicology, College of Veterinary Medicine and BK21 Program for Veterinary Science
Seoul National University, Seoul 151-744 (Korea)
Fax: (+82) 2-873-1268
E-mail: mchotox@snu.ac.kr

Dr. S. M. Jin,[+] I. Yang, Prof. Dr. S. K. Kim
School of Chemistry
Seoul National University, Seoul 151-744 (Korea)

Prof. Dr. J. H. Lee
Department of Radiology, Samsung Medical Center
School of Medicine, Sungkyunkwan University
Seoul 137-200 (Korea)

[+] Present address:
Advanced Materials Division
Korea Research Institute of Chemical Technology
Daejeon 305-343 (Korea)

[§] These authors contributed equally to this work.

[**] T.H. acknowledges financial support by the Korean Ministry of Science and Technology through the National Creative Research Initiative Program of the Korea Science and Engineering Foundation (KOSEF). M.H.C. is supported by the NSI-NCRC program of KOSEF. S.K.K. is supported by a National Research Laboratory Grant and a Chemical Genomics Grant. J.H.L. is supported by the Centre for Biological Modulators of the 21st Century Frontier R&D Program.

Supporting information for this article (experimental details, demonstration of the rapid destruction of cancer cells by irradiation with a femtosecond-pulse laser, and the temporal distribution of the output power for a femtosecond-pulse laser versus that of a continuous-wave laser) is available on the WWW under http://www.angewandte.org or from the author.

Molecular imaging using magnetic resonance imaging (MRI) is an emerging technology that can be used to image target tissues in vivo in a highly specific manner. Iron oxide nanoparticles, such as superparamagnetic iron oxide (SPIO) nanoparticles, have been extensively utilized as MRI contrast agents for molecular imaging.[4]

Recently, a great deal of attention has been paid to noninvasive photothermal therapy for the selective treatment of tumor cells. This type of therapy utilizes the large absorption cross section of nanomaterials in the near infrared (NIR) region. Owing to its weak absorption by tissues, NIR radiation is able to penetrate the skin without causing much damage to normal tissues and, thus, can be used to treat specific cells targeted by the nanomaterials. Several nanomaterials that strongly absorb NIR radiation, including gold nanoshells,[5] gold nanorods,[6] and single-walled carbon nanotubes,[7] were recently demonstrated to have potential therapeutic applications. The radiation that is absorbed by these nanomaterials is converted efficiently into heat, causing cell destruction on a picosecond time scale, as a result of electron–phonon and phonon–phonon processes.[5–8]

The clever combination of different nanoscale materials can lead to the development of multifunctional nanomedical platforms for simultaneous targeted delivery, fast diagnosis, and efficient therapy.[9] For example, Kopelman and coworkers reported multifunctional nanoparticles for the simultaneous targeted photodynamic therapy and in vivo MRI of a rat brain cancer;[9f] these polyacrylamide nanoparticles contained photosensitizers and MRI contrast agents, and their surfaces were coated with poly(ethylene glycol) (PEG) and molecular targeting groups. We herein propose that nanostructures with combined magnetic and optical properties can provide a novel nanomedical platform for diagnostic imaging, using the magnetic properties, and simultaneous treatment, using the optical properties. With this goal in mind, we fabricated magnetic gold nanoshells (Mag-GNS) consisting of gold nanoshells embedded with magnetic Fe_3O_4 nanoparticles, and conjugated them with a cancer-targeting agent. Cancer cells targeted by these Mag-GNS can be detected by a clinical MRI system and killed by NIR radiation. Femtosecond laser pulses are particularly useful in the selective, efficient, and rapid destruction of the targeted cancer cells.

The synthetic approach is represented in Figure 1a, and transmission electron microscope (TEM) images of the products obtained after each synthetic step are shown in Figure 1b–e. In this synthetic method, Fe_3O_4 (magnetite) nanoparticles and gold seed nanoparticles are assembled on amino-modified silica spheres;[10] gold shells are then grown around the silica spheres (see Supporting Information).[11] First, 100-nm silica spheres were synthesized using the Stöber method,[12] and the surfaces of the particles were modified with 3-aminopropyltrimethoxysilane (Figure 1b). Monodisperse 7-nm Fe_3O_4 nanoparticles stabilized with oleic acid were synthesized[13] and subsequently ligand-exchanged with 2-bromo-2-methylpropionic acid (BMPA).[14] The BMPA-stabilized Fe_3O_4 nanoparticles were then covalently attached to the amino-modified silica spheres through a direct nucleophilic substitution reaction between the bromo groups and the amino groups (Figure 1c).[15] Gold seed nanoparticles of 1–3 nm[16] were attached to the residual amino groups of the silica spheres (Figure 1d). Finally, a complete 15-nm-thick gold shell with embedded Fe_3O_4 nanoparticles was formed around the silica spheres, resulting in Mag-GNS (Figure 1e). Recently, similarly structured gold nanoshells embedded with magnetite nanoparticles were fabricated by Mirkin and coworkers.[17]

Figure 2a shows that the Mag-GNS are deep purple in color and disperse well in water. In the Vis/NIR spectrum of the Mag-GNS, an absorption band ranging from 700 nm to the NIR region is observed (Figure 2b). The field-dependent magnetization curve of the Mag-GNS at 300 K shows no hysteresis (Figure 2c), which is consistent with superpara-

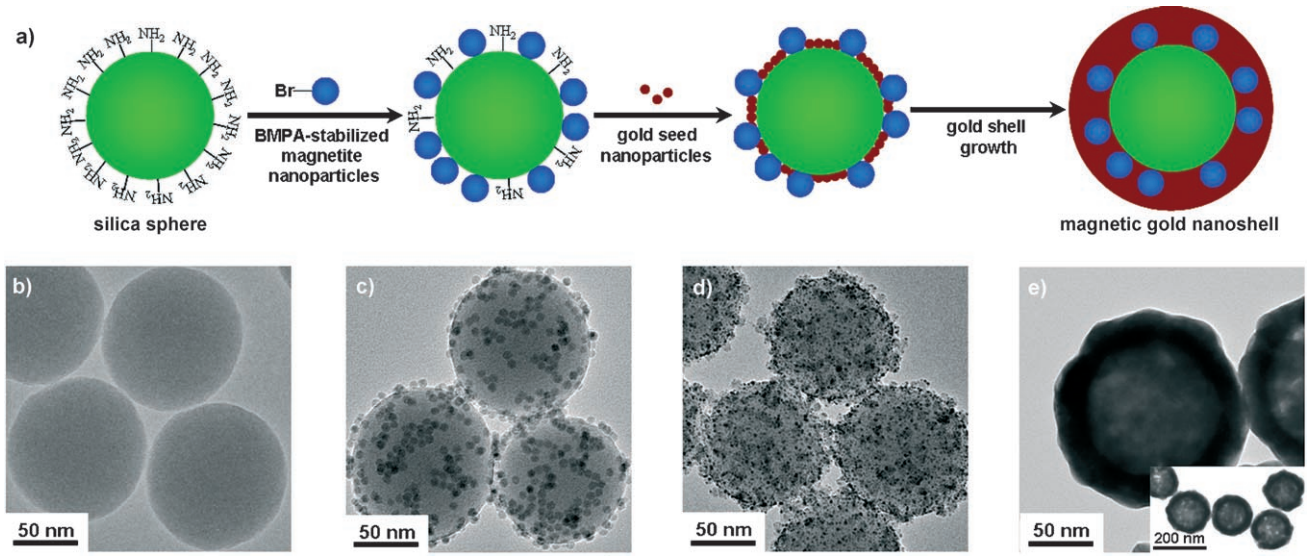

Figure 1. a) Synthesis of the magnetic gold nanoshells (Mag-GNS). TEM images of b) amino-modified silica spheres, c) silica spheres with Fe_3O_4 (magnetite) nanoparticles immobilized on their surfaces, d) silica spheres with Fe_3O_4 and gold nanoparticles immobilized on their surfaces, and e) the Mag-GNS.

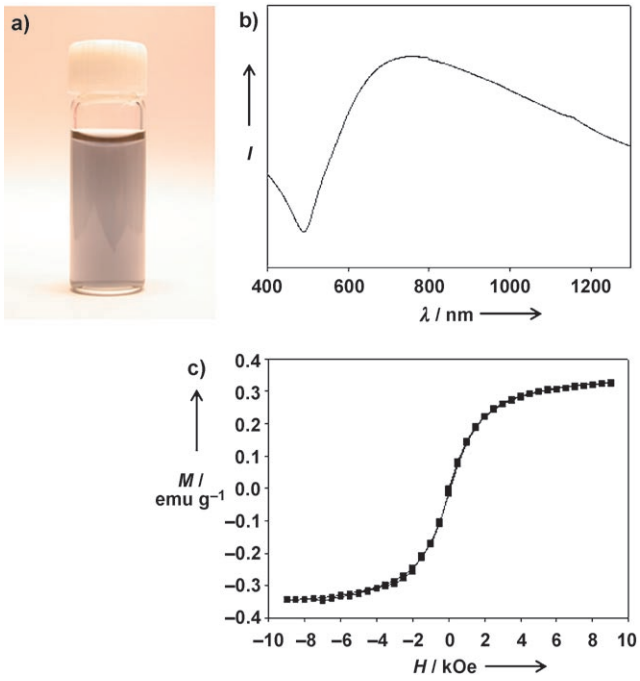

Figure 2. a) Photograph of the Mag-GNS dispersed in water. b) Vis/NIR spectrum of the Mag-GNS. c) Field dependence of the magnetization of the Mag-GNS at 300 K.

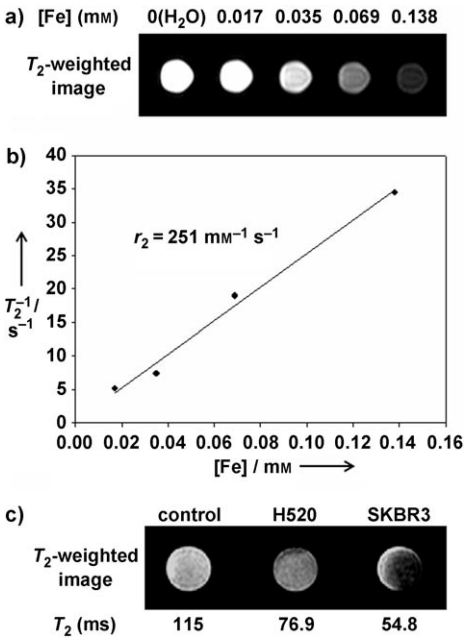

Figure 3. a) T_2-weighted MR images of the PEG-coated Mag-GNS at various concentrations in water. b) Plot of the spin–spin relaxation rate (T_2^{-1}) against iron concentration for the PEG-coated Mag-GNS, from which the specific relaxivity (r_2) is determined. c) T_2-weighted MR images of control SKBR3 cells, HER2/*neu*-negative H520 cells incubated with Mag-GNS-$Ab_{HER2/neu}$, and HER2/*neu*-positive SKBR3 cells incubated with Mag-GNS-$Ab_{HER2/neu}$; the corresponding T_2 relaxation times are indicated.

magnetic behavior arising from the embedded magnetite nanoparticles.

The Fe_3O_4 nanoparticles have a tendency to shorten the spin–spin relaxation times (T_2) of water, resulting in a decrease in the MRI signal intensity.[4] MR images of the PEG-coated Mag-GNS at various concentrations in water are shown in Figure 3a. As the concentration of the PEG-coated Mag-GNS increases, the signal intensity of the MR image decreases, owing to the presence of the embedded Fe_3O_4 nanoparticles. This behavior allows the Mag-GNS to be used as a T_2 contrast agent. The specific relaxivity, which is a measure of the change in the spin–spin relaxation rate (T_2^{-1}) per unit concentration, is $r_2 = 251\ mM^{-1}s^{-1}$ for the PEG-coated Mag-GNS (Figure 3b).

For targeted MRI and NIR photothermal therapy, we conjugated an antibody, anti-HER2/*neu* ($Ab_{HER2/neu}$), onto the surface of the Mag-GNS using a PEG linker (see Supporting Information), to prepare Mag-GNS that target the HER2/*neu* receptors of the breast cancer cells (Mag-GNS-$Ab_{HER2/neu}$). HER2/*neu*-positive SKBR3 breast cancer cells and HER2/*neu*-negative H520 lung cancer cells[18] were incubated with Mag-GNS-$Ab_{HER2/neu}$ for 2 h at 37 °C (see Supporting Information). T_2-weighted MR images were recorded for the SKBR3 and H520 cells treated with Mag-GNS-$Ab_{HER2/neu}$, as well as for untreated control SKBR3 cells, on a 3.0-T clinical MRI system (Figure 3c; see Supporting Information). The T_2-weighted MR image of the Mag-GNS-$Ab_{HER2/neu}$-treated SKBR3 cells was much darker than those of the Mag-GNS-$Ab_{HER2/neu}$-treated H520 cells and the control SKBR3 cells. The T_2 relaxation times of the Mag-GNS-$Ab_{HER2/neu}$-treated SKBR3 and H520 cells, and the control SKBR3 cells were 54.8, 76.9, and 115 ms, respectively. Thus, the Mag-GNS can be a contrast agent in targeted MRI for the detection of cancer cells.

Results of targeted NIR photothermal therapy against cancer cells using Mag-GNS-$Ab_{HER2/neu}$ are presented in Figure 4 (see Supporting Information). The Mag-GNS-$Ab_{HER2/neu}$-treated SKBR3 and H520 cells, and the control SKBR3 cells were exposed to a femtosecond-pulse laser with a wavelength of 800 nm and a beam diameter of 1 mm for 10 s. The power of the laser was varied from 20–80 mW in steps of 10 mW. After exposure to the NIR laser, the dead cells were stained blue by treating them with 0.4% trypan blue for 10 min. No destruction of the control SKBR3 cells was observed, even after exposure to a power of 80 mW (Figure 4a). The death of the Mag-GNS-$Ab_{HER2/neu}$-treated H520 cell began at 60 mW (Figure 4b). However, in the case of the Mag-GNS-$Ab_{HER2/neu}$-treated SKBR3 cells, cell death was observed even at a low power of 20 mW (Figure 4c). These results clearly demonstrate that the Mag-GNS-$Ab_{HER2/neu}$, which absorb NIR radiation, were more effectively targeted on the SKBR3 cells than on the H520 cells, because of a strong antigen–antibody interaction in the SKBR3 cells. At 20 mW, only the SKBR3 cells at the center of the laser beam were exposed to the high intensity of the femtosecond pulse, which has a Gaussian distribution, and thus destroyed. With increasing laser power, the area of the dead cells spread. The cells burst and died as a result of the local heating generated by the absorption of NIR radiation by the Mag-GNS-$Ab_{HER2/neu}$. The control SKBR3 cells, which stayed alive, exhibited normal morphology after exposure to a power of

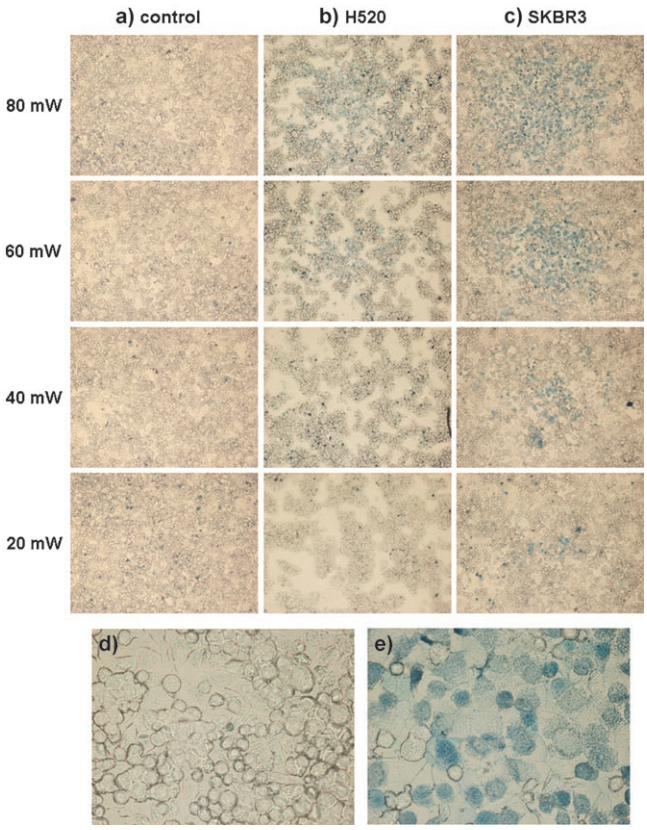

Figure 4. Optical microscope images of a) control SKBR3 cells, b) HER2/*neu*-negative H520 cells incubated with Mag-GNS-$Ab_{HER2/neu}$, and c) HER2/*neu*-positive SKBR3 cells incubated with Mag-GNS-$Ab_{HER2/neu}$ after irradiation for 10 s with a femtosecond-pulse laser (with a wavelength of 800 nm and a beam diameter of 1 mm) at various intensities and subsequent staining with trypan blue. High-magnification optical microscope images of d) control SKBR3 cells and e) SKBR3 cells incubated with Mag-GNS-$Ab_{HER2/neu}$ after irradiation at a power of 80 mW and subsequent staining.

80 mW (Figure 4d), whereas most of the Mag-GNS-$Ab_{HER2/neu}$-treated SKBR3 cells were burst, and the cytoplasm of the dead cells stained by trypan blue spread to the medium (Figure 4e).

The use of a femtosecond-pulse laser is crucial to this experiment.[19] Although the average power of a femtosecond-pulse laser may be comparable with that of a continuous-wave (CW) laser, its peak power greatly exceeds that of the CW laser.[20] The large amount of energy tightly packed in the femtosecond pulses imparts an enormous impact on the sample, both temporally and spatially.[21] Furthermore, the duration of a femtosecond pulse is much shorter than the characteristic time for relaxation through intermolecular energy transfer,[22] preventing the dissipation of the photon energy and, thus, resulting in very effective local heating by photo-excitation. These characteristics of the femtosecond pulse lead to a unique feature that could have an important implication for in vivo therapy: the photodegradation of the cancer cells is greatly accelerated, and thus, the required dose of radiation is correspondingly reduced. For example, irradiation for only 10 s is necessary for the destruction of the SKBR3 cells with a femtosecond-pulse laser, whereas 2–7 min is normally required with a CW laser at a similar or higher intensity.[5–7]

Recently, several multifunctional nanomedical platforms have been reported.[9] The probes encapsulated by biologically localized embedding (PEBBLEs) produced by the Kopelman group are particularly interesting, because different types of photosensitizers, imaging contrast agents, and targeting agents can be simultaneously incorporated into polymer or silica nanoparticles.[9f] Although the multifunctional nanomedical features of PEBBLEs are similar to those of our Mag-GNS, there are several key differences between these two nanomaterials. Firstly, the compositions are completely different. Our Mag-GNS consist of a silica nanosphere core surrounded by a gold nanoshell for photothermal therapy, with embedded magnetite nanoparticles for T_2 MRI contrast enhancement. In contrast, the PEBBLEs consist of polyacrylamide nanoparticles containing organic dyes for photodynamic therapy and gadolinium complexes for T_1 MRI contrast enhancement. Secondly, cancer cells are killed by the two nanomaterials through different mechanisms. In photothermal therapy using Mag-GNS, the NIR radiation absorbed by the gold nanoshells is converted efficiently into a sufficient amount of heat to kill cancer cells. In contrast, in photodynamic therapy using PEBBLEs,[9f] reactive oxygen species generated by laser irradiation of the photosensitizers kill the cancer cells. Thirdly, the Mag-GNS absorb NIR radiation, which is optimal for the treatment of deep tissues, because the absorption of NIR radiation in tissues is generally much less than that of visible light, and consequently tissue penetration is enhanced. Fourthly, irradiation of the cancer-targeting Mag-GNS-$Ab_{HER2/neu}$ using a femtosecond-pulse laser with an NIR wavelength makes it possible to kill cancer cells at a low power and in a short period of time. This very effective destruction of cancer cells through localized heating by photo-excitation results from the synergetic effects of the femtosecond laser pulse and the NIR irradiation.

In conclusion, multifunctional Mag-GNS consisting of gold nanoshells with embedded magnetic Fe_3O_4 nanoparticles were synthesized. Anti-HER2/*neu* was linked to the Mag-GNS for targeted MRI and NIR photothermal therapy of cancer cells. The embedded Fe_3O_4 nanoparticles resulted in high contrast in the MR images, and the gold nanoshells had an optical absorption cross section high enough for NIR photothermal therapy. Cancer cells targeted with the Mag-GNS-$Ab_{HER2/neu}$ in vitro were detectable by a commercial clinical MRI system, and were rapidly destroyed upon short exposure to femtosecond laser pulses with an NIR wavelength and a low power.

Received: June 20, 2006
Revised: August 21, 2006
Published online: October 30, 2006

Keywords: gold · magnetic resonance imaging · nanomedicine · nanostructures · photothermal therapy

[1] a) C. M. Niemeyer, C. A. Mirkin, *Nanobiotechnology: Concepts, Applications and Perspectives*, Wiley-VCH, Weinheim, **2004**; b) U. Häfeli, W. Schütt, J. Teller, M. Zborowski, *Scientific and Clinical Applications of Magnetic Carriers*, Plenum, New York, **1997**; c) P. Alivisatos, *Nat. Biotechnol.* **2004**, *22*, 47; d) K. J. Klabunde, *Nanoscale Materials in Chemistry*, Wiley-Interscience, New York, **2001**; e) T. Hyeon, *Chem. Commun.* **2003**, 923; f) A. L. Rogach, D. V. Talapin, E. V. Shevchenko, A. Kornowski, M. Haase, H. Weller, *Adv. Funct. Mater.* **2002**, *12*, 653; g) A. P. Alivisatos, *Science* **1996**, *271*, 933; h) C. B. Murray, C. R. Kagan, M. G. Bawendi, *Annu. Rev. Mater. Sci.* **2000**, *30*, 545.

[2] a) M. Bruchez, Jr., M. Moronne, P. Gin, S. Weiss, A. P. Alivisatos, *Science* **1998**, *281*, 2013; b) W. C. W. Chan, S. Nie, *Science* **1998**, *281*, 2016; c) S. Kim, Y. T. Lim, E. G. Soltesz, A. M. De Grand, J. Lee, A. Nakayama, J. A. Parker, T. Mihaljevic, R. G. Laurence, D. M. Dor, L. H. Cohn, M. G. Bawendi, J. V. Frangioni, *Nat. Biotechnol.* **2004**, *22*, 93; d) I. L. Medintz, H. T. Uyeda, E. R. Goldman, H. Mattoussi, *Nat. Mater.* **2005**, *4*, 435; e) X. Gao, Y. Cui, R. M. Levenson, L. W. K. Chung, S. Nie, *Nat. Biotechnol.* **2004**, *22*, 969.

[3] a) T. A. Taton, C. A. Mirkin, R. L. Letsinger, *Science* **2000**, *289*, 1757; b) J.-M. Nam, C. S. Thaxton, C. A. Mirkin, *Science* **2003**, *301*, 1884; c) D. G. Georganopoulou, L. Chang, J.-M. Nam, C. S. Thaxton, E. J. Mufson, W. L. Klein, C. A. Mirkin, *Proc. Natl. Acad. Sci. USA* **2005**, *102*, 2273.

[4] a) J. W. M. Bulte, D. L. Kraitchman, *NMR Biomed.* **2004**, *17*, 484; b) L. Josephson, C.-H. Tung, A. Moore, R. Weissleder, *Bioconjugate Chem.* **1999**, *10*, 186; c) M. Zhao, D. A. Beauregard, L. Loizou, B. Davletov, K. M. Brindle, *Nat. Med.* **2001**, *7*, 1241; d) H. W. Kang, L. Josephson, A. Petrovsky, R. Weissleder, A. Bogdanov, Jr., *Bioconjugate Chem.* **2002**, *13*, 122; e) R. Weissleder, A. Moore, U. Mahmood, R. Bhorade, H. Benveniste, E. A. Chiocca, J. P. Basilion, *Nat. Med.* **2000**, *6*, 351; f) J. M. Perez, L. Josephson, T. O'Loughlin, D. Högemann, R. Weissleder, *Nat. Biotechnol.* **2002**, *20*, 816; g) J. W. M. Bulte, S.-C. Zhang, P. van Gelderen, V. Herynek, E. K. Jordan, I. D. Duncan, J. A. Frank, *Proc. Natl. Acad. Sci. USA* **1999**, *96*, 15256.

[5] a) C. Loo, A. Lowery, N. J. Halas, J. L. West, R. Drezek, *Nano Lett.* **2005**, *5*, 709; b) D. P. O'Neal, L. R. Hirsch, N. J. Halas, J. D. Payne, J. L. West, *Cancer Lett.* **2004**, *209*, 171; c) L. R. Hirsch, R. J. Stafford, J. A. Bankson, S. R. Sershen, B. Rivera, R. E. Price, J. D. Hazle, N. J. Halas, J. L. West, *Proc. Natl. Acad. Sci. USA* **2003**, *100*, 13549.

[6] X. Huang, I. H. El-Sayed, W. Qian, M. A. El-Sayed, *J. Am. Chem. Soc.* **2006**, *128*, 2115.

[7] N. W. S. Kam, M. O'Connell, J. A. Wisdom, H. Dai, *Proc. Natl. Acad. Sci. USA* **2005**, *102*, 11600.

[8] S. Link, M. A. El-Sayed, *Int. Rev. Phys. Chem.* **2000**, *19*, 409.

[9] a) L. Levy, Y. Sahoo, K.-S. Kim, E. J. Bergey, P. N. Prasad, *Chem. Mater.* **2002**, *14*, 3715; b) G. Zheng, J. Chen, H. Li, J. D. Glickson, *Proc. Natl. Acad. Sci. USA* **2005**, *102*, 17757; c) E. Garanger, D. Boturyn, Z. Jin, P. Dumy, M.-C. Favrot, J.-L. Coll, *Mol. Ther.* **2005**, *12*, 1168; d) I. J. Majoros, T. P. Thomas, C. B. Mehta, J. R. Baker, Jr., *J. Med. Chem.* **2005**, *48*, 5892; e) I. J. Majoros, A. Myc, T. Thomas, C. B. Mehta, J. R. Baker, Jr., *Biomacromolecules* **2006**, *7*, 572; f) R. Kopelman, Y.-E. L. Koo, M. Philbert, B. A. Moffat, G. R. Reddy, P. McConville, D. E. Hall, T. L. Chenevert, M. S. Bhojani, S. M. Buck, A. Rehemtulla, B. D. Ross, *J. Magn. Magn. Mater.* **2005**, *293*, 404; g) H. Xu, S. M. Buck, R. Kopelman, M. A. Philbert, M. Brasuel, B. D. Ross, A. Rehemtulla, *Isr. J. Chem.* **2004**, *44*, 317; h) F. Yan, H. Xu, J. Anker, R. Kopelman, B. Ross, A. Rehemtulla, R. Reddy, *J. Nanosci. Nanotechnol.* **2004**, *4*, 72; i) J. Kim, J. E. Lee, J. Lee, J. H. Yu, B. C. Kim, K. An, Y. Hwang, C.-H. Shin, J.-G. Park, J. Kim, T. Hyeon, *J. Am. Chem. Soc.* **2006**, *128*, 688.

[10] J. Kim, J. E. Lee, J. Lee, Y. Jang, S.-W. Kim, K. An, J. H. Yu, T. Hyeon, *Angew. Chem.* **2006**, *118*, 4907; *Angew. Chem. Int. Ed.* **2006**, *45*, 4789.

[11] a) S. J. Oldenburg, R. D. Averitt, S. L. Westcott, N. J. Halas, *Chem. Phys. Lett.* **1998**, *288*, 243; b) C. Graf, A. van Blaaderen, *Langmuir* **2002**, *18*, 524.

[12] W. Stöber, A. Fink, E. Bohn, *J. Colloid Interface Sci.* **1968**, *26*, 62.

[13] J. Park, K. An, Y. Hwang, J.-G. Park, H.-J. Noh, J.-Y. Kim, J.-H. Park, N.-M. Hwang, T. Hyeon, *Nat. Mater.* **2004**, *3*, 891.

[14] Y. Wang, X. Teng, J.-S. Wang, H. Yang, *Nano Lett.* **2003**, *3*, 789.

[15] a) K. Ha, Y.-J. Lee, H. J. Lee, K. B. Yoon, *Adv. Mater.* **2000**, *12*, 1114; b) S.-S. Bae, D. K. Lim, J.-I. Park, W.-R. Lee, J. Cheon, S. Kim, *J. Phys. Chem. B* **2004**, *108*, 2575.

[16] D. G. Duff, A. Baiker, P. P. Edwards, *Langmuir* **1993**, *9*, 2301.

[17] S. I. Stoeva, F. Huo, J.-S. Lee, C. A. Mirkin, *J. Am. Chem. Soc.* **2005**, *127*, 15362.

[18] P. A. Bunn, Jr., B. Helfrich, A. F. Soriano, W. A. Franklin, M. Varella-Garcia, F. R. Hirsch, A. Baron, C. Zeng, D. C. Chan, *Clin. Cancer Res.* **2001**, *7*, 3239.

[19] M. Sawa, K. Awazu, T. Takahashi, H. Sakaguchi, H. Horiike, M. Ohji, Y. Tano, *Br. J. Ophthalmol.* **2004**, *88*, 826.

[20] a) A. E. Siegman, *Lasers*, University Science Books, Sausalito, **1986**; b) O. Svelto, *Principles of Lasers*, Plenum, New York, **1998**.

[21] a) M. E. Fermann, A. Galvanauskas, G. Sucha, *Ultrafast Lasers: Technology and Application*, Marcel Dekker, New York, **2002**; b) W. Kaiser, *Ultrashort Laser Pulses: Generation and Application*, Springer, New York, **1993**.

[22] N. J. Turro, *Modern Molecular Photochemistry*, University Science Books, Sausalito, **1991**.

